Investigation of Feasibility of Using Low-Cost AHRS Devices to Detect General Aviation Hazardous States

Conference Paper · June 2019

DOI: 10.2514/6.2019-3444

Nicoletta Fala
Purdue University

Investigation of Feasibility of Using Low-Cost AHRS Devices to Detect General Aviation Hazardous States

Arpan Chakraborty,[1] Nicoletta Fala[1] and Karen Marais[2]
Purdue University, West Lafayette, IN, 47907

General Aviation (GA) accidents constitute most of aviation related accidents. Flight data analysis has helped reduce the accident rate in commercial aviation. Similarly, safety analysis based on flight data can help GA be safer. However, GA aircraft flight data recorders are costly. Low-cost flight recorders are few and rarely used in GA safety analysis due to lack of accuracy compared to certified on-board equipment. In this paper we investigate the feasibility of using a low cost AHRS to detect hazardous states in GA aircraft. We consider the case of roll angles and, using flight data, find that the low-cost device has significant measurement errors. We develop models to correct the roll angle error as well as methods to improve the detection of hazardous roll angles. We observe that the models to improve the roll angle do not improve hazardous state detection. However, redefining the hazardous limit for the low-cost AHRS increases detection probability.

I. Nomenclature

GA = General Aviation
AHRS = Attitude and Heading Reference System
FAA = Federal Aviation Administration
FOQA = Flight Operational Quality Assurance
FDM = Flight Data Management
IMU = Inertial Measurement Unit
GNSS = Global Navigation Satellite System
GPS = Global Positioning System
ADS-B = Automatic Dependent Surveillance-Broadcast
HS = Hazardous State
MD = Missed Detection
FA = False Alarms
RMSE = Root Mean Square Error
PDF = Probability Density Function
CDF = Cumulative Density Function
RL = Risk Level
RC = Risk Category
IR = Integration Results

II. Introduction

Flight Operational Quality Assurance (FOQA), or Flight Data Management (FDM), has played a role in commercial aviation since the 1960s. FOQA is a voluntary safety program through which commercial airlines and pilots share de-identified aggregated information with the FAA so that the FAA can monitor national trends in aircraft operations and address operational risk issues [[1]]. Airlines with an active FDM program have accident rates that are 50% lower than carriers without FOQA, and carriers that have used FOQA for the longest also have the fewest accidents [2]. The FOQA philosophy could help decrease the large number of GA accidents [3]. However, FOQA for

[1] Graduate Research Assistant, School of Aeronautics and Astronautics, 701 W. Stadium Ave, Student Member
[2] Associate Professor and Associate Head for Undergraduate Education, School of Aeronautics and Astronautics, 701 W. Stadium Ave, Associate Fellow.

GA faces several roadblocks. Most GA aircraft are not equipped with flight recorders [4]. On-board Electronic Flight Instrument Systems (EFIS) can record aircraft data, but only newer GA aircraft are equipped with EFIS. Most GA pilots are owner operators, and unlike airline operators, the financial return on investment in expensive in-flight data recorders is not necessarily obvious.

Independent Flight Data Recorders (iFDR), also known as Lightweight Aircraft Recording Systems, do not connect to existing on-board aircraft systems, but rather collect flight data using their own sensors. iFDRs include recording devices such as mounted cameras to record cockpit instruments and engine noise recordings. These devices can store large amounts of data, but this data requires extensive post-processing. Several Electronic Flight Bag (EFB) applications can also record GPS, traffic, and weather data, but they require external Attitude Heading and Reference Systems (AHRS) to provide aircraft orientation. Pilots can connect commercial portable AHRS devices to the handheld device system applications and potentially record data, but these devices cost approximately $1,000 per system.

GA safety analyses in the literature primarily use EFIS flight data. EFIS flight data from GA aircraft include GPS data, Attitude and Heading Reference System (AHRS) data, communication/navigation information, and engine information. Previous safety analyses have used Garmin G1000 EFIS data to identify phases of flight [5], to detect safety events during the approach phase of flight [6], and to detect anomalies in GA operations [7], and the Vision 1000 camera to record and flight tests for a helicopter [8].

Several researchers have investigated the use of low-cost sensors to collect flight data in GA. Researchers have used low-cost sensor data for aircraft simulator validation [9], angle-of-attack derivation [10], altitude measurements [11], and to generate an operating handbook for experimental aircraft [12]. The question remains: Can we use the data collected via low-cost sensors for GA safety analysis in the same manner as the data used from an EFIS such as the Garmin G1000?

Here, we investigate the feasibility of using the data from a Stratux to (1) collect GA flight data (roll angle, ϕ) and (2) detect GA high roll angles. Section III describes the low cost AHRS (Stratux) unit and our data collection approach. In Section IV we assess the Stratux's ability to detect high roll angles ($\phi > 45°$) compared to the on-board certified G1000 and develop and test post-processing algorithms to improve the detection performance of the Stratux.

III. Stratux Data Collection and Processing

An AHRS is a complex system consisting of an IMU, a microprocessor, and a GPS unit. We investigated the available low-cost AHRS options for GA [14] and acquired a low-cost device (a Stratux) that GA pilots currently use and is easy to build. The Stratux is a low-cost ADS-B In receiver and AHRS unit with open-source software that pilots can build on their own.

To compare the performance of the Stratux data to the G1000 data, we built a Stratux device (shown in Fig. 1 (a)) and created an Android application to collect GPS and aircraft attitude data from the Stratux. We then collected data from the Stratux (using the Android application) and the G1000 (by downloading EFIS data directly from the aircraft) on training flights in a Cirrus SR-20 at Purdue University. We placed the Stratux, an external battery pack, and an Android smartphone in the baggage compartment of three identical aircraft and collected data from 29 training flights. To ensure valid and consistent data across the three aircraft and all the flights, we strapped all equipment on a Styrofoam mount (shown in Fig. 1 (b)), which helped align the Stratux with the longitudinal axis of the airplane before each flight.

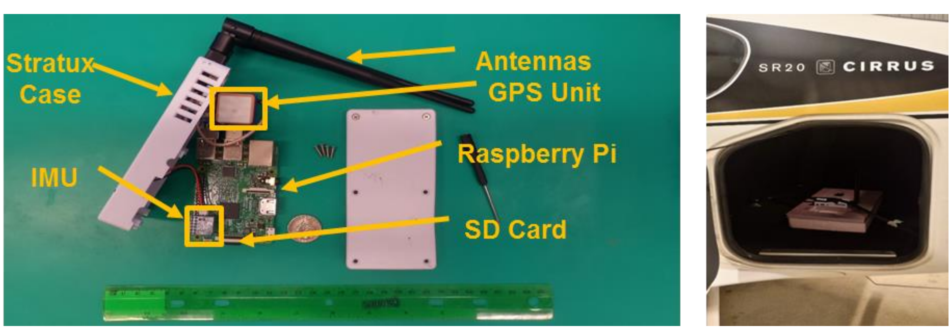

Fig. 1: The Stratux unit we built (a) consists of a Raspberry Pi microcontroller, two antennae, a GPS unit, an IMU, and an SD card containing the software. We created a mount (b) to ensure consistent measurements in all flight tests and placed it in the baggage area of a Cirrus SR-20.

The data collected from the 29 training flights consists of cross-country flights as well as flight maneuver lessons at the private and commercial pilot level. The bank angle in these flights varied from mostly straight and level in the case of cross-country flights to 45° or more during maneuvers such as steep turns and steep spirals. In the remainder of this paper, we will refer to individual flights by flight number, ranging from Flight 1 to Flight 29.

IV. Detecting High Roll Angle

Roll angle (also known as bank angle), φ, describes the attitude of the aircraft about its longitudinal axis. The roll angle influences safety-critical flight parameters such as stall speed and sideslip and is an important flight parameter in determining the state of the aircraft. A state is a time segment wherein a system exhibits a particular behavior. A hazardous state is a system state that may lead to an accident or an incident if corrective action is not taken [13]. A high roll angle (ϕ) is an example of such a hazardous state, since sustaining a high roll angle could cause a stall. For example, in 2017 a Cirrus SR-22 airplane crashed while on a right turn to the final approach leg to runway 32 at the Stinson Municipal Airport in San Antonio, Texas. The aircraft was approaching the runway at a calibrated airspeed of 103 knots, at 200 feet above the ground, and at an approximate roll angle of 48°, when it started descending at more than 1,800 fpm. The report concluded that the aircraft crashed due to the aircraft stalling at high roll angle and excessive side slip [15].

In this section, we first analyze the performance of the Stratux device in recording roll angle by comparing it to the G1000. We then describe two methods of improving the use of Statux data in safety analysis. First, we try to reduce the error in Stratux roll angle measurements by using statistical models to adjust the Stratux roll angles so that they match the G1000 roll angles. Second, we accept the Stratux roll angles as they are recorded, and instead adjust our safety analysis to work better with erroneous data, by switching our hard limits that define a hazardous state to soft limits that include a margin of error.

A. Initial Performance Analysis

Pilots of aircraft without an EFIS cannot go back and investigate the safety of their flight after landing. Low-cost data, if accurate, could give those pilots tools to improve their safety. However, low-cost data is erroneous, compared to the Garmin G1000 data, which we consider to be our ground truth in this research. Like any measurement device, the G1000 also has errors, but it is a certified system and previous researchers have used the G1000 data for GA safety analysis [5], [6], [7]. Therefore, we compared the Stratux roll angles to the G1000 roll angles, as shown in Fig. 2 [14], to evaluate how the error is distributed. In section IV.B, we present some ways to minimize the error.

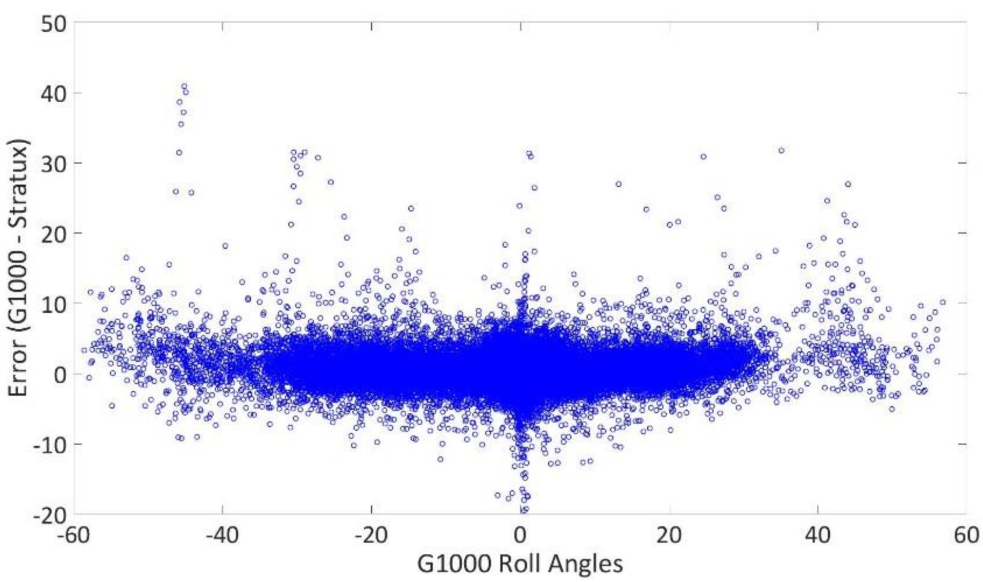

Fig. 2: Both the Garmin G1000 and the Stratux unit record roll angle. There is a high variation in the error between the G1000 and the Stratux roll angles, and it is not symmetric about 0°.

We define a roll angle limit based on the Private Pilot-Airman Certification Standards, which use a hard limit of 45° for banking maneuvers such as steep turns [16]. A "Missed Detection" (MD) occurs when the Stratux records a roll angle of magnitude of less than 45°, but the G1000 roll angle magnitude is greater than 45°. Conversely, if the Stratux roll angle magnitude is greater than 45° and the G1000 roll angle magnitude less than 45°, then the Stratux had a "False Alarm" (FA). Fig. 3 shows the flights that included high roll angles according to the G1000 data. The Stratux missed nearly half of the hazardous states in Flight 1 and Flight 7, and almost all the hazardous states in Flight 3 and Flight 5. In section IV.0, we modify the limit definitions to reduce the number of missed detections and false alarms.

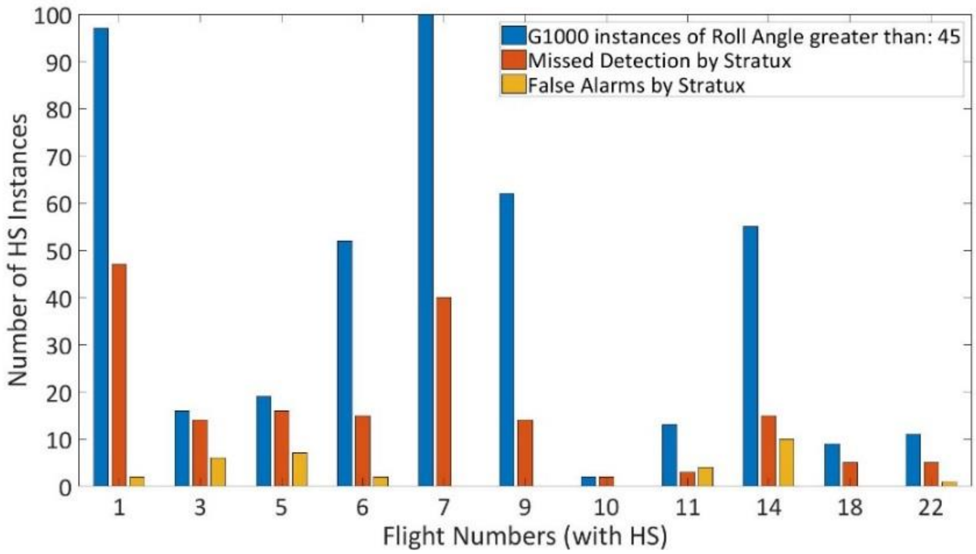

Fig. 3: The Stratux does not perform the same way as the Garmin G1000. Assuming that the G1000 records the true values, the Stratux misses some detections (such as in Flight 1 and 7) and detects some false alarms (such as in Flight 14).

Overall, the Stratux correctly identifies about ~53% of hazardous states. We expected the Stratux to perform poorly in detecting hazardous states due to the large errors shown in Fig. 2. Previous studies in automobile traffic information systems suggest that an accuracy level of less than 40% is not accurate enough to support user acceptance, but that 60% may be [21]. Therefore, we need to either reduce the errors in the Stratux roll angles or change the definition of the hazardous limit applied to the Stratux to have better detection accuracy when using the Stratux.

B. Reducing Stratux roll angle error

To reduce the errors in the Stratux angles, we used three different models: (1) a continuous linear model that maps the Stratux roll angles directly to the G1000 roll angles, (2) piecewise transfer functions to model the error and then adjust the Stratux roll angles, and (3) piecewise polynomials that map the Stratux roll angles directly to the G1000 roll angles.

1. Model 1: Continuous Linear Model

We used a continuous linear model to adjust the Stratux roll angle as shown by Equation (1) and the linear fit in Fig. 4 to fit the Stratux roll angle data to the G1000 roll angle data.

$$\phi_{adjusted} = a \cdot \phi_{Stratux} + c \tag{1}$$

The coefficients $a = 1.009$ and $c = 0.1276$ provided a fit with an *RMSE* value of 1.7762 and $r^2 = 0.9563$, which is a good statistical fit. However, the Stratux and G1000 roll data are unequally distributed across roll angles. We have more data points for smaller roll angles than for larger roll angles. The relatively good statistics of the linear fit are due to the large number of data points at smaller angles.

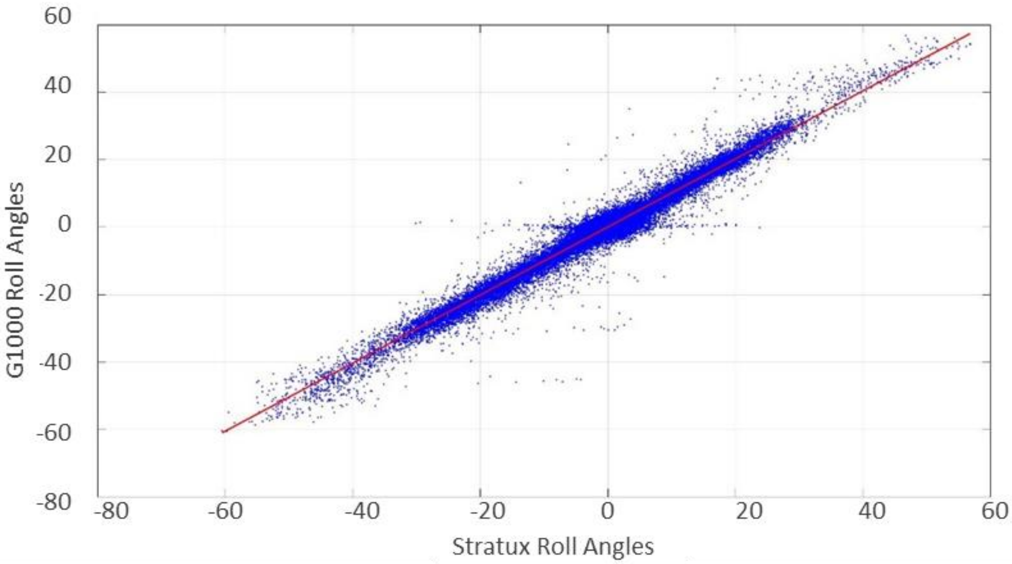

Fig. 4: The Single Linear Model fits the G1000 roll angle data well, however, the statistical fit is biased by the large number of data points at small angles.

2. Model 2: Piecewise Fourier Transfer functions

To create piecewise Fourier transfer functions, we split the range of the Stratux roll data into thirteen 10° intervals from −65° to +65° and modeled the error between the Stratux and G1000 roll angles, as shown in Fig. 5. Models for each interval are independent of one another, piecewise, and discontinuous. Equation (2) shows the Fourier transfer function type that captures the error characteristics. The number of function parameters increases for intervals where the error is larger. Equation (3) adds the estimated error from Equation (2) to the Stratux angle to get the adjusted angle. We add the improved error estimate back to the observed Stratux angle to find the improved Stratux roll angle:

$$error_{adjusted} = a_0 + a_1 \times \cos(w \times \phi_{Stratux}) + b_1 \times \sin(w \times \phi_{Stratux}) + \cdots \tag{2}$$

$$\phi_{adjusted} = \phi_{Stratux} + error_{adjusted} \tag{3}$$

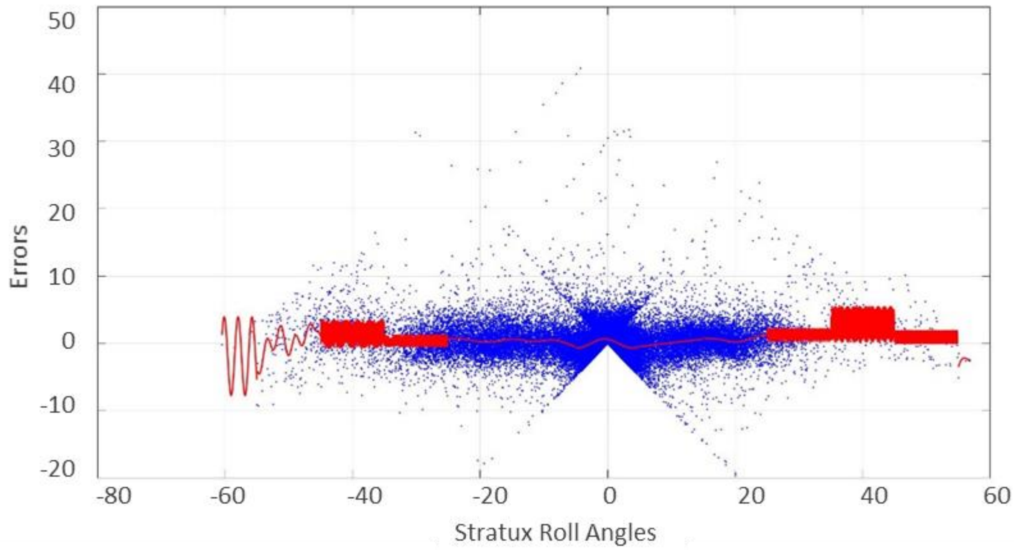

Fig. 5: We modeled the error between the Stratux and G1000 roll angle data using piecewise Fourier transforms for intervals of 10°. The larger error variations and lack of data at larger angles cause the increasing transfer function amplitudes.

3. Model 3: Piecewise Polynomial functions

In Model 3 we modify the Stratux roll to directly mimic G1000 roll angles, unlike Model 2, where we used the error to find the improved Stratux angle indirectly. Similar to Model 2, we split the Stratux roll angles into thirteen intervals from −65° to +65° of 10° each. Equation (4) shows the polynomial function type for each of the thirteen intervals. As with Model 2, all polynomial models for each interval are independent of each other, piecewise, and discontinuous. Fig. 6 shows the thirteen models for each interval. The order of the polynomial increases for higher magnitude angles because they have larger errors and there are fewer data points.

$$\phi_{adjusted} = p_0 + (p_1 \times \phi_{Stratux}) + (p_2 \times \phi_{Stratux}^2) + (p_3 \times \phi_{Stratux}^3) + \cdots \tag{4}$$

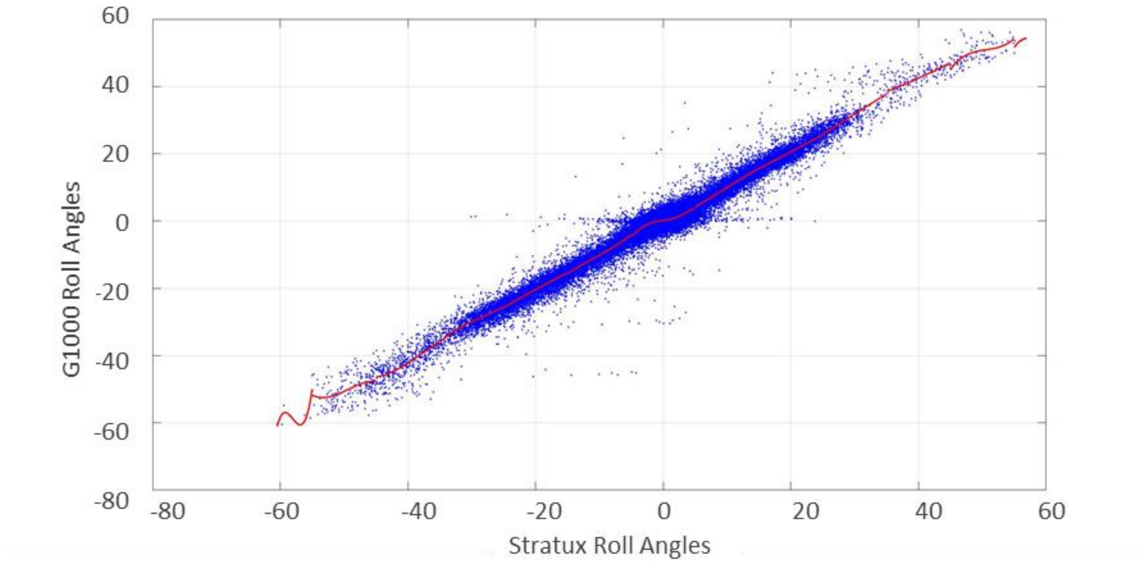

Fig. 6: The degree of the polynomial fit is greater at larger angles where we have less data.

4. Results on Training Set

Table 1 compares Missed Detections and False Alarms between the unmodified Stratux values and the three models discussed in this section for all the flights that had at least one instance of the hazardous state. Model 1, despite being a statistically good fit, does not improve the detection of high roll angles as it cannot improve the Stratux roll angle values at large angles. The piecewise models (Models 2 and 3) reduce the number of missed detections but increase false alarms. Since the piecewise models show improvements, we choose Model 3 for further investigation. In Section **Error! Reference source not found.** we test the piecewise polynomial model on a new set of flight data.

Table 1: Model 1 did not improve hazardous state detection. Both piecewise models (Models 2 and 3) reduced the number of missed detections and increased false alarms.

Flight identifier	Unmodified Stratux Roll Angle Data		Model 1: Continuous Linear Fit		Model 2: Piecewise Fourier Transfer Function Model		Model 3: Piecewise Polynomial Function Model	
	MD	FA	MD	FA	MD	FA	MD	FA
1	47	2	42	4	29	14	27	13
3	14	6	13	9	8	25	8	26
5	16	7	16	7	12	17	12	20
6	15	2	15	2	11	3	11	3
7	40	0	39	0	21	3	21	3
9	14	0	12	0	3	0	5	1
10	2	0	2	0	0	1	0	1
12	15	10	14	14	7	19	9	22
16	5	0	2	0	0	1	0	1
19	5	1	5	1	2	3	1	3

C. Changing the Roll Angle Safety Limits for Stratux

When comparing the roll angle detection accuracy of the Stratux to the G1000, we used 45° as a hard roll angle limit with no error buffer. For example, if the G1000 angle was 45.1° and the Stratux was 45°, we considered the Stratux to have missed the detection. We also know that the Stratux roll angles are erroneous compared to the G1000 roll angles. To account for the Stratux error, we adjust the hard limits, and refer to these adjusted limits as "soft" limits. We define the hazardous state soft limits for the Stratux as shown in Equation (5).

$$Soft\ Limit\ =\ Hard\ Limit\ \pm\ \mu_{Error} \tag{5}$$

Fig. 7 shows the soft limits about the hard limits of +45° and −45°. We refer to the lower magnitude limits as the inner soft limit and the higher magnitude limits as the outer soft limit. Since the error distribution is not symmetric about 0°, the same hard limit for negative and positive roll angles translates to different soft limits.

Using Equation (5), we redefine the 'Missed Detection and 'False Alarm' errors based on the soft limits for +45° and −45°:

- If the G1000 roll angle magnitude is greater than |45°| and the Stratux roll angle magnitude is less than |45°|, but greater than the magnitude of the inner soft limit, then we cannot be certain that the Stratux missed detecting a hazardous state.
- If the G1000 roll angle magnitude is less than |45°| and the Stratux roll angle magnitude is greater than |45°|, but less than the magnitude of the outer soft limit, then we cannot be certain that the Stratux has falsely detected a hazardous state.

Fig. 7 shows the instances where the bank angle (as recorded by the G1000) was close to crossing the hard limit in one of the flights (Flight 5). For ease of visualization, we have removed time from the x-axis, so each instance is not necessarily equally spaced in time. The solid black lines indicate the hard limits and the dashed black lines indicate the soft limits. The zones of uncertainty are marked by translucent red bands. We consider the Stratux angles that lie within the red bands to be correct detections.

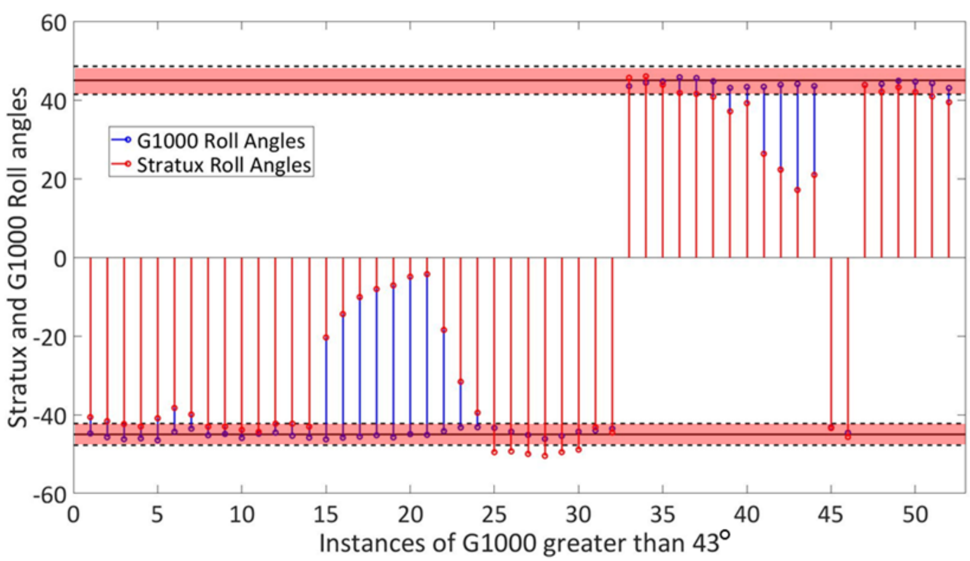

Fig. 7: In this sample flight (Flight 5), we changed the hard limits to soft limits, shown by the red bands. Angles that fall in the red band are considered correct detections of the hazardous state.

Fig. 8 shows the results for missed detections and false alarms for each flight where a hazardous state occurred, using the unmodified Stratux bank angle data and soft limits for hazardous state detection, resulting in a decrease in both missed detections and false alarms.

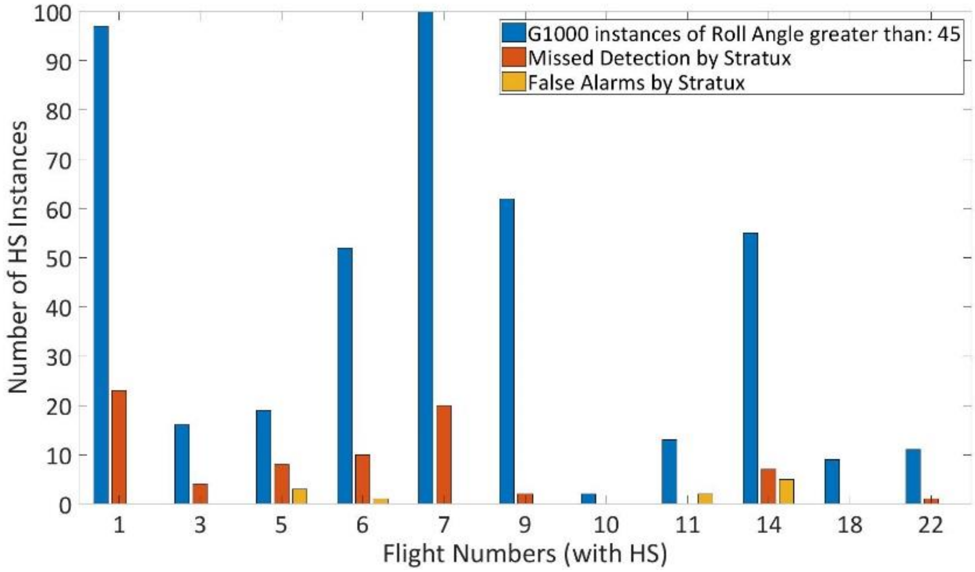

Fig. 8: Using soft limits on unmodified data decreased the number of both missed detections and false alarms.

V. Probability of Detecting Hazardous States Correctly (ϕ > 45°)

In this section, we define two types of hazardous state detection probabilities: (1) the probability that the Stratux data correctly detects a hazardous state given that the G1000 data indicates a hazardous state (section V.A) and (2) the probability that a hazardous state exists in the G1000 data for a specific Stratux angle (section V.B). These two probabilities describe the relative accuracy of hazardous state detection using the Stratux compared to the G1000. In section V.C, we test our improved detection methods on a set of five new flights to evaluate if the probability of correct detection increases.

A. Probability of the Stratux data detecting a G1000 Hazardous State

We treat detections of hazardous states as discrete independent events. A detection is a success and a missed detection or false alarm is a failure. Previous studies have shown that nuisance alarms can decrease user trust in the system or lead to operators ignoring the alarms [17][18]. We use Equation (6) to find the number of correct detections (CD) of the hazardous state. If the Stratux roll angle data correctly indicates all the instances of the G1000 hazardous states but has additional false alarms, then the CD of the Stratux drops.

$$CD = (Instances\ of\ HS)_{G1000} - MD_{Stratux} - FA_{Stratux} \tag{6}$$

We find the probability of the Stratux data correctly identifying a hazardous state (HS) given that the G1000 has detected a hazardous state, i.e., p($HS_{Stratux}$ |HS_{G1000}) and the 95% confidence interval of the probability using the Clopper-Pearson method [19]. When we use the unmodified Stratux roll angles and the hard limit of 45°, the probability of correct detection for the Stratux is 0.5229 with a 95% confidence interval of (0.4749 − 0.5707).

B. Probability of Hazardous State Occurring at Different Stratux Angles

Since the Stratux error varies with angle, the probability of observing a hazardous state for a given Stratux angle also varies. Here, we find the probability of a hazardous state (*HS*) occurring (according to the G1000) for an observed Stratux angle, i.e. p(HS_{G1000} |$\phi_{Stratux}$).

For example, if the Stratux records an angle of 40°, and the defined limit is 45° then the possibilities are:

- The G1000 roll angle is greater than +45° or less than −45° and a hazardous state has occurred.
- The G1000 roll angle is less than |45°| and no hazardous state has occurred.

We developed probability density functions (PDFs) of the G1000 roll angles for a 1° range of the Stratux roll angles spanning from –60° to +60°. Fig. 9 shows the PDF for +40° ≤ $Roll_{Stratux}$ <+ 41° and the area under the curve for a hazardous state (ϕ > |45°|).

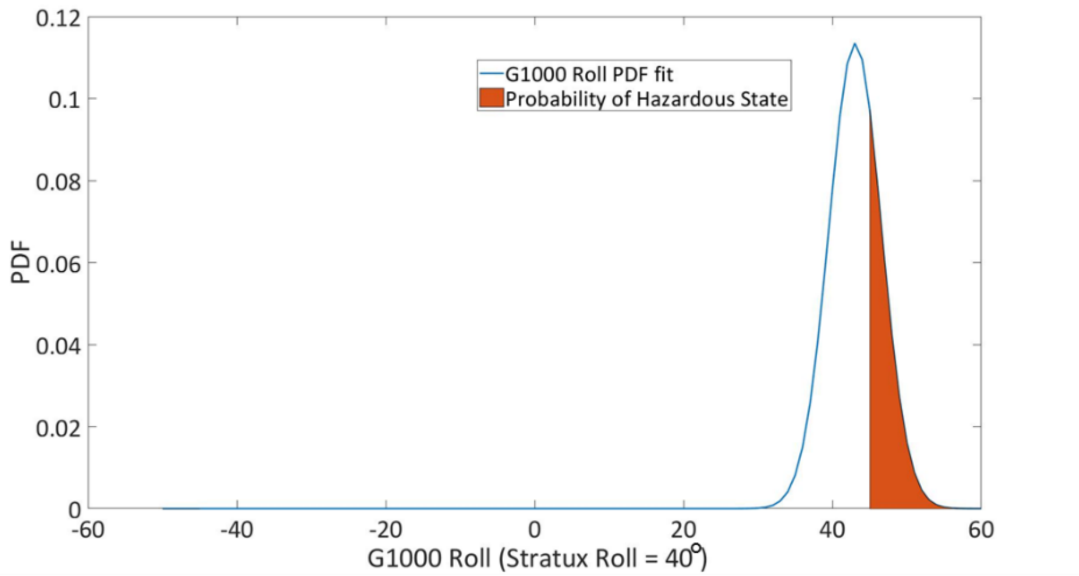

Fig. 9: The curve shows the probability density function of the G1000 roll angles for which the unmodified Stratux angle is 40°. The area under the curve beyond the hard limit of 45° is the probability of a hazardous state occurring.

In Fig. 10, the solid red line indicates the "Ideal Probability" of detecting the hazardous state. This probability is zero between −45° and +45° and one beyond the limits. The probability of a hazardous state for a given Stratux angle (40° in Fig. 9) is the area under the PDF in Fig. 9. The blue line with markers in Fig. 10 is the probability for each Stratux angle based on the flight data. The probability of the hazardous state is the sum of the cumulative density function (CDF) at −45° and (1 – CDF) at +45°.

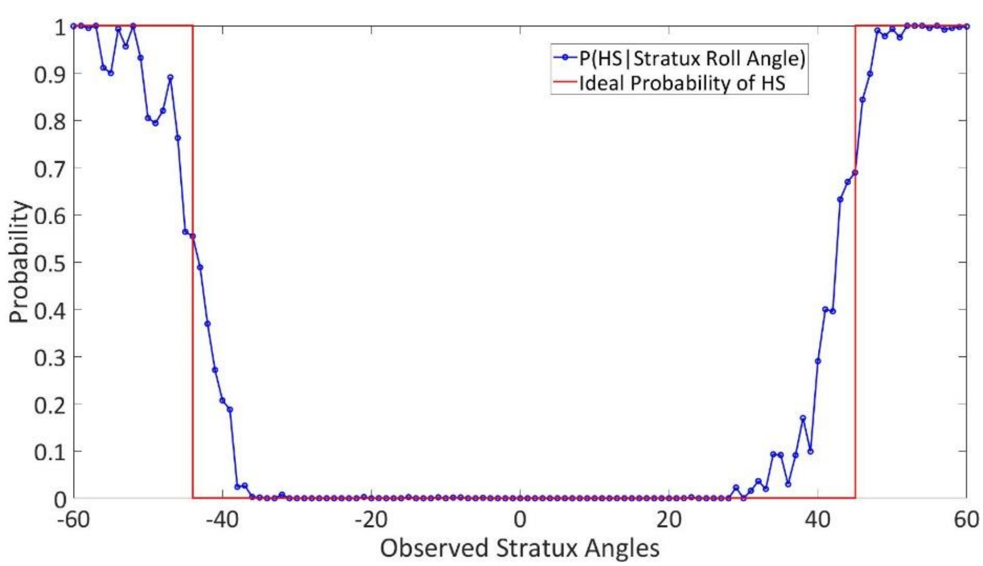

Fig. 10: Ideally, the probability of a hazardous state occurring when the Stratux angle is between -45° and 45° should be zero. The probability should be one otherwise, resulting in a step function. However, because the Stratux values are erroneous, the probability does not follow exactly a step function.

C. Improving Hazardous State Detection using Adjusted Stratux Measurements and Adjusted Hazardous State Definition Limits

In Section IV, we developed models that improve the Stratux roll angles so that they match the G1000 data, and used soft limits to detect hazardous states. In this section, we calculate the probabilities of correctly detecting hazardous roll angle and test our approach on five new flights.

Table 2 shows the number of missed detections, false alarms, and correct detections for the unmodified and improved Stratux with hard and soft limits for five test flights. The improved Stratux roll angles reduced missed detections but increased false alarms. The soft limits improved correct detection overall.

Table 2: In the five test flights, the adjusted Stratux data reduced the number of missed detections, but increased false alarms. Switching to soft limits reduced missed detections and false alarms, leading to improved correct detection overall.

Unmodified Stratux data with Hard Limit			Adjusted Stratux data with Hard Limit			Unmodified Stratux data with Soft Limits			Adjusted Stratux data with Soft Limits		
MD	**FA**	**CD**	**MD**	**FA**	**CD**	**MD**	**FA**	**CD**	**MD**	**FA**	**CD**
3	4	6	0	7	6	0	1	12	0	2	11

In the dataset of five test flights, a hazardous roll angle state (ϕ > 45°) only occurred thirteen times. These occurrences are insufficient to evaluate whether the improved Stratux and/or soft limits improve hazardous state detection. Our purpose here is to assess *how well* our method detects anomalous behavior, rather than detecting HS in these particular flights. However, since our data is all from supervised training flights, there are few instances of roll angles larger than 45°. Therefore, to allow us to evaluate our method, we define a new hazardous roll angle limit based on the anomalous behavior in our test data set. This approach is similar to how unstable approaches are defined [20]. In our test set, 95% of the roll angles are at or below an absolute value of 19°, so we set a new hazardous state limit to 19°.

We used the methods described in sub-sections A and B to find the probabilities of the Stratux correctly identifying roll angles having a magnitude greater than 19°. Table 3 shows the probabilities of detection of roll angles greater than 19° for the unmodified and improved Stratux data with hard and soft limits. The Stratux roll angle error varies [14], but the error is lower at lower magnitude angles than at higher magnitude angles. Since the hazardous limit we are using here is smaller than the previous limit of 45°, the probability of detection for the actual Stratux is higher than the value of 0.52 we found in sub-section A. The values in Table 3 also indicate that the model-improved Stratux roll angle has little impact on overall correct detection. The soft limits, however, increase the correct detection probability by 10%.

Table 3: The statistical models meant to match the Stratux roll angle data to the G1000 data did little to improve the overall correct detection on the five test flights. However, the soft limits increase the correct detection probability by 10%.

	Hard Limit and Unmodified Stratux data	Hard Limit and Improved Stratux data	Soft Limits and Unmodified Stratux data	Soft Limits and Improved Stratux data
Probability of Correct Detection	0.8308	0.8333	0.9160	0.9336
95% CI of Probability	0.8030 – 0.8562	0.8056 – 0.8585	0.8946 – 0.9343	0.9140 – 0.9499

Next, we assess the performance of our methods across a range of hazardous roll angles, from |20°| to |59°|. We use the same 24 flights as before to train the models, and test them on the same remaining five flights.

In Fig. 11 and Fig. 12, the cyan and the magenta plot lines indicate the detection probabilities when we use the soft limits for the Stratux. The magenta line also indicates the probabilities for the improved Stratux roll angles similarly to the red line, which indicates the improved Stratux roll angles without the soft limits. The blue line is the unmodified Stratux roll angle detection probabilities without the soft limits. The improved Stratux roll angles reduce the number of missed detections, but also increase the number of false alarms and do not improve upon the overall correct detection. Furthermore, at high magnitude angles the Stratux roll angles are highly erroneous and the models we created using the training data do not correct for the errors in the test data.

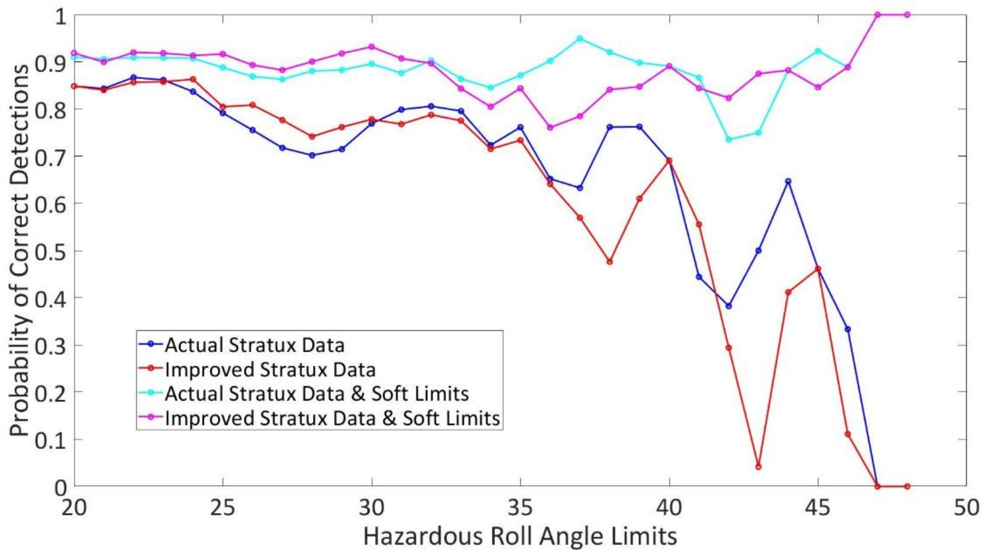

Fig. 11: As the definition for a hazardous roll angle increases, the probability that we detect it correctly tends to decrease. The improvements made to the Stratux data did not perform well on the test data (compared to the training data in Fig. 12) and did not increase the probability of correct detection. The largest roll angle in the test set was 48°, compared to 59° in the training set.

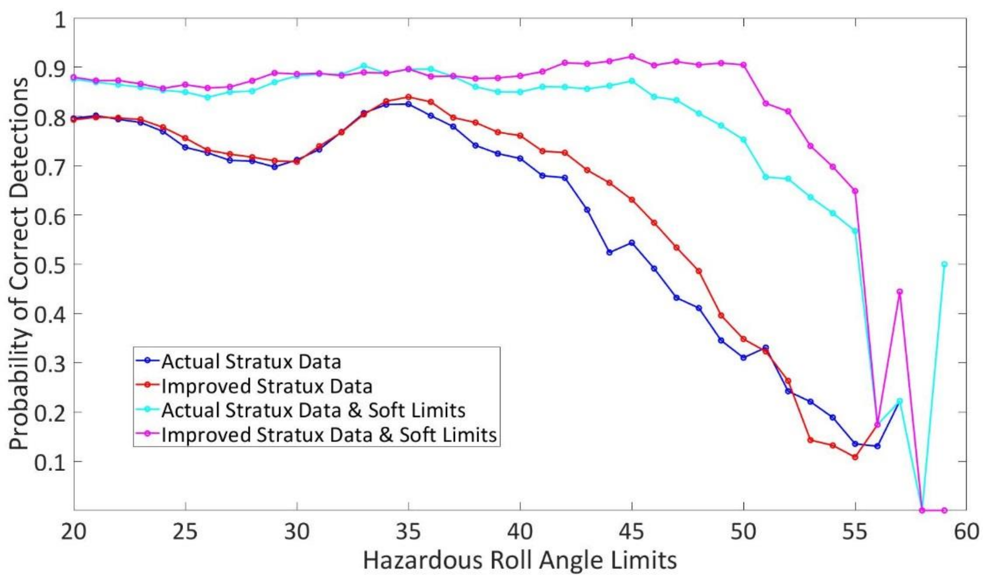

Fig. 12: As expected, the improvements made to the Stratux data performed better on the training data than the test data (Fig. 11). However, even with the training data, adjusting the Stratux roll angles only marginally improved the probability of correct detection. Using soft limits to detect hazardous states performed a lot better, with high probability of correct detection even at 45° and beyond.

When using hard limits, the probability of correct detection is above 60% for all hazardous state definitions until 40°, and below 60% for definitions greater than 40°.

As shown in Fig. 11 and Fig. 12, applying the soft limits always improves the detection of the roll angles larger than the defined limit. The soft limits we developed from the training set ensure that the correct detection probability of the unmodified Stratux roll angles in the test data set remains above 70% for all roll angle limits ranging from |20°| to |48°|. Using the soft limits in the training data, the probability of the unmodified Stratux roll angles correctly detecting larger angles than the defined limit is above 80% for angles ranging from |20°| to |48°|. In the training set, the probability of correct detection when using soft limits remains above 60% till |54°|.

VI. Conclusion and Future Work

Using our Stratux device, we collected flight data using an Android application. Compared to the G1000, the Stratux data missed 48% of the roll angles greater than 45° in our training set. Previous studies in automobile traffic information systems suggest that an accuracy level of 40% is not accurate enough to support user acceptance, but that 60% likely is [21]. Therefore, we developed two methods to increase the detection probability of angles beyond a hazardous roll angle limit when using the Stratux: (1) use piecewise-discontinuous models to improve the Stratux roll angles and match that of the G1000, and (2) modify the hazardous roll angle limit to soft limits for the Stratux. Piecewise-discontinuous models of the Stratux roll angle reduced the number of missed detections but increased the number of false alarms. Increasing false alarms can lead to a decrease in user trust [17], and when we incorporated false alarms in correct detection probability (equation (6), we found that the models we used to improve the Stratux roll angles in this research did not increase the detection probability of the Stratux. However, using soft limits substantially increases the detection probability of the Stratux for any definition of hazardous roll angle limit.

In our research, we used the Private Pilots' rolling maneuver limit of 45°. The FAA's GA Aviation Safety Information Analysis and Sharing (ASIAS) program can help in providing data to better determine the roll angle limit for safe operations. We investigated a hazardous state based on a single flight parameter, but aircraft hazardous states are complex and depend on multiple dependent variables. For example, roll angle and speed: the stalling speed of an aircraft increases with the increase in roll angle. We will need to investigate the methods discussed in this research when applied to more than one variable defining a hazardous state, such as, roll angle and airspeed. The data collected in this research is from a single Stratux. To validate the methods and results we present in this research, we will need to apply the methods to additional low cost AHRS devices. Additionally, we can find the optimum models for the Stratux roll angles.

Acknowledgments

This research was partially funded by the US Department of Transportation/Federal Aviation Administration PEGASAS Center of Excellence under Award No 12-C-GA-PU AM44, 55. The project was managed by Michael Vu.

The views expressed in this paper are those of the authors and do not necessarily reflect those of the FAA. The information in this research does not constitute FAA Flight Standards or FAA Aircraft Certification policy.

Leonardo Vilela Teixeira, Jianfei Gao, and Prof. Bruno Ribeiro of the Computer Science department at Purdue University supported the Android Application development for the Stratux data collection.

References

[1] Federal Aviation Administration, "Flight Operational Quality Assurance," Advisory Circular, AC No: 120-82, April 2004

[2] Lau K. S., "General Aviation Flight Data Monitoring, Fly with Intelligence – Best Practices to Improve the Safety and Efficiency of Flight Operations," CAPACG White Paper, March 2007.

[3] Federal Aviation Administration, "Fact Sheet – General Aviation Safety," URL: https://www.faa.gov/news/fact_sheets/news_story.cfm?newsId=21274 [retrieved 30 September 2018].

[4] Federal Aviation Administration, "Flight data recorders and cockpit voice recorders," Electronic Code of Federal Regulations, 14 CFR §91.609," URL: https://www.ecfr.gov/cgi-bin/text-idx?node=14:2.0.1.3.10#sp14.2.91.g [retrieved 06 November 2018].

[5] Goblet, V., Fala, N., and Marais, K., "Identifying Phases of Flight in General Aviation Operations," 15th AIAA Aviation Technology, Integration, and Operations Conference, 2015.

[6] Fala, N., and Marais, K., "Detecting Safety Events during Approach in General Aviation Operations," 16th AIAA Aviation Technology, Integration, and Operations Conference, 2016.

[7] Puranik, G. T., Mavris, N. D., "Anomaly Detection in General-Aviation Operations Using Energy Metrics and Flight-Data Records," Journal of Aerospace Information Systems, Vol. 15, No. 1, January 2018.

[8] Kuo, C. B., Guan, W., and Chen, P., "In Search of General Aviation Flight Data Monitoring: Lightweight Recording System," 17th AIAA Aviation Technology, Integration, and Operations Conference, 2017.

[9] Neuhart, A. R., Gingras, R. D., Hultberg, S. R., Oltman, S. R., and Graybeal, W. N., "Flight Data Collection for General Aviation Aircraft Simulation Validation," AIAA Atmospheric Flight Mechanics Conference, 10 - 13 August 2009.

[10] Valasek, J., Harris, J., Pruchnicki, S., McCrink, M., Gregory, J., and Sizoo, G. D., "Characterization of Derived Angle-of-Attack and Sideslip Angle Algorithms Using Monte Carlo and Piloted Simulation," AIAA Atmospheric Flight Mechanics Conference, 5-9 June 2017.

[11] Albéri, M., Baldoncini, M., Bottardi, C., Chiarelli, E., Fiorentini, G., Giulia, K., Raptis, C., Realini, E., Reguzzoni, M., Rossi, L., Sampietro, D., Strati, V., and Mantovani, F., "Accuracy of Flight Altitude Measured with Low-Cost GNSS, Radar and Barometer Sensors: Implications for Airborne Radiometric Surveys," Sensors 2017.
[12] Bonadonna, C., Brody, D., Lopez, A., "Design of a Low-Cost General Aviation Flight Data Recording and Analysis System," 2015 IEEE Systems and Information Engineering Design Symposium, 2015.
[13] Rao, H. A., and Marais, K., "Comparing Hazardous States and Trigger Events in Fatal and Non-Fatal Helicopter Accidents," 16th AIAA Aviation Technology, Integration, and Operations Conference, 2016.
[14] Chakraborty, A., "Detecting GA Aircraft Hazardous States Using A Low-Cost Attitude and Heading Reference System," MS Thesis, School Aeronautics and Astronautics, Purdue University, West Lafayette, Indiana, December 2018 (unpublished).
[15] National Transportation Safety Board, "Aviation Accident Factual Report," Accident Number: CEN17FA084, 2018.
[16] Federal Aviation Administration, "Private Pilot- Airman Certification Standards," June 2018.
[17] Cafarelli, A. D., "Effect of False Alarm Rate on Pilot Use and Trust of Automation under Conditions of Simulated High Risk", MS Thesis, Aeronautics and Astronautics, Massachusetts Institute of Technology, September 1998.
[18] William, L. M., "False Alarms Buffet Pilots, Air Controllers", Los Angeles Times, April 1998, URL: http://articles.latimes.com/1998/apr/06/news/mn-36621 [retrieved 30 November, 2018].
[19] Clopper, J. C., and Pearson, S. E., "The Use of Confidence or Fiducial Limits Illustrated in the Case of the Binomial,", Biometrika, Vol. 26, No. 4., pp. 404-413, December 1934.
[20] Jiao, Y., Sun, H., Wang, C., and Han, J. (2018), "Research on Unstable Approach Detection of Civil Aviation Aircraft", 8th International Congress of Information and Communication Technology (ICICT-2018).
[21] Fox, J., "The effects of age and ATIS congestion information accuracy on user trust and compliance," Ph.D. Thesis, Department of Psychology, George Mason University, 1998.